

# The Contribution of Conformational Adjustments and Long-range Electrostatic Forces to the CD2/CD58 Interaction\*

Received for publication, January 29, 2007, and in revised form, March 7, 2007 Published, JBC Papers in Press, March 7, 2007, DOI 10.1074/jbc.M700829200

Alice Kearney<sup>‡1</sup>, Adam Avramovic<sup>‡</sup>, Mónica A. A. Castro<sup>§¶12</sup>, Alexandre M. Carmo<sup>¶12</sup>, Simon J. Davis<sup>§3</sup>, and P. Anton van der Merwe<sup>‡1,4</sup>

From the <sup>‡</sup>Sir William Dunn School of Pathology, University of Oxford, Oxford OX1 3RE, United Kingdom, <sup>§</sup>Medical Research Council Human Immunology Unit, Weatherall Institute of Molecular Medicine, Nuffield Department of Clinical Medicine, University of Oxford, Oxford OX3 9DS, United Kingdom, and <sup>¶</sup>Group of Cell Activation and Gene Expression, Instituto de Biologia Molecular e Celular and Instituto de Ciências Biomédicas de Abel Salazar, Universidade do Porto, 4099-002 Porto, Portugal

CD2 is a T cell surface molecule that enhances T and natural killer cell function by binding its ligands CD58 (humans) and CD48 (rodents) on antigen-presenting or target cells. Here we show that the CD2/CD58 interaction is enthalpically driven and accompanied by unfavorable entropic changes. Taken together with structural studies, this indicates that binding is accompanied by energetically significant conformational adjustments. Despite having a highly charged binding interface, neither the affinity nor the rate constants of the CD2/CD58 interaction were affected by changes in ionic strength, indicating that long-range electrostatic forces make no net contribution to binding.

The CD2 family of cell-surface glycoproteins are structurally related members of the Ig superfamily (1, 2). Expressed mainly on hematopoietic cells, they modulate immune responses by homotypic or heterotypic interactions with other members of the CD2 family. CD2 binds CD58 (in humans) or CD48 (in rodents), and these interactions enhance T cell recognition of antigen on antigen-presenting or target cells. This enhancement is thought to involve both adhesion and signaling mechanisms (1, 3–7).

CD2 and its interaction with its ligands have been studied intensively and have emerged as an important paradigm for understanding the molecular basis of cell-cell recognition (1, 8, 9). CD2 and its ligands have structurally related ectodomains comprised of two Ig domains, with the membrane-distal domains involved in ligand binding (1, 8). The interaction of human CD2 with CD58 is characterized by low affinity ( $K_d \sim 10 \mu\text{M}$  at 37 °C), which is the result of a very fast dissociation rate constant ( $k_{\text{off}} > 4 \text{ s}^{-1}$ ) (10). Structural studies of the individual proteins and site-directed mutagenesis locate the binding sites on the equivalent GFCC'C'  $\beta$ -sheets of CD2 and CD58 and reveal them to be highly charged (11–13). Solution of the crystal structure of the complex between the human CD2 and CD58 ligand binding domains provides a detailed view of the binding

interface (14). This is relatively small (buried surface area  $\sim 1160 \text{ \AA}^2$ ) and has poor surface-shape complementarity, consistent with the low affinity (14). Comparison of the structure of the complex with the structure of unbound CD2 (15–17) and CD58 (12, 13) reveals significant differences, particularly in the case of CD2. The most prominent differences are in the C'C' and FG loops of both molecules (14, 16). In addition NMR analysis shows that the CD58 binding site on unbound CD2 is highly flexible, with most of the movement occurring in the C'C' and FG loops (16, 17). Taken together, these data suggest CD2 binding to CD58 is accompanied by conformational adjustment and stabilization of a flexible interface. Although these conformational changes provide an explanation for the low affinity of the CD2/CD58 interaction, they appear to be inconsistent with its relatively fast  $k_{\text{on}}$  (10).

To further investigate these putative conformational changes and the discrepancy between the structural and kinetic data, we undertook a detailed thermodynamic and kinetic analysis of the CD2/CD58 interaction. We show here that the interaction is enthalpically driven and accompanied by unfavorable entropic changes, consistent with stabilization of a flexible binding interface. We also show that, despite having a highly charged binding interface, long-range electrostatic interactions have no net effect on the CD2/CD58 interaction.

## EXPERIMENTAL PROCEDURES

**Proteins**—Soluble forms of CD2 and CD58 were prepared and purified as described previously (18). These comprised the full ectodomains with C-terminal oligohistidine tags. The C termini of the encoded CD2 and CD58 were SCPEKHHHHHH and TCIPSSHHHHHH, respectively.

**Surface Plasmon Resonance**—These studies were performed on a BIAcore 2000 (BIAcore AB) (19). Unless otherwise stated, experiments were performed at 25 °C using HBS buffer (10 mM HEPES (pH 7.4), 150 mM NaCl, 1 mM  $\text{CaCl}_2$ , and 1 mM  $\text{MgCl}_2$ ) at a flow rate of  $10 \mu\text{l} \cdot \text{min}^{-1}$ . Human CD2 was directly coupled to research grade CM5 sensor chips (BIAcore AB) using the amine coupling kit (BIAcore) as described previously (10). Kinetics measurements were performed at a flow rate of  $50 \mu\text{l} \cdot \text{min}^{-1}$  and confirmed at three different immobilization levels of CD2 to rule out mass transport artifacts.

Affinity, kinetic, and thermodynamic properties were determined as described (20). Equilibrium thermodynamic parameters were obtained by measuring the affinity over a range of

\* The costs of publication of this article were defrayed in part by the payment of page charges. This article must therefore be hereby marked "advertisement" in accordance with 18 U.S.C. Section 1734 solely to indicate this fact.

<sup>1</sup> Supported by the Medical Research Council, United Kingdom.

<sup>2</sup> Supported by the European Regional Development Fund (FEDR) and Fundação para a Ciência e a Tecnologia.

<sup>3</sup> Supported by the Wellcome Trust.

<sup>4</sup> To whom correspondence should be addressed. Tel.: 44-1865-274493; Fax: 44-1865-274491; E-mail: anton.vandermerwe@path.ox.ac.uk.

temperatures (5–37 °C) and fitting the nonlinear form of the van't Hoff equation to these data (21),  $\Delta G = \Delta H_{T_0} - T\Delta S + \Delta C_p(T - T_0) - T\Delta C_p \ln(T/T_0)$ , where  $T$  is the temperature (in degrees Kelvin),  $T_0$  is an arbitrary reference temperature (e.g. 298.15 K),  $\Delta G$  is the free energy of binding at the standard state (all components at 1 mol·liter<sup>-1</sup>),  $\Delta H_{T_0}$  is the enthalpy change at  $T_0$  (kcal·mol<sup>-1</sup>),  $\Delta C_p$  is the heat capacity change (kcal·mol<sup>-1</sup>K<sup>-1</sup>) at constant pressure, and  $\Delta S$  is the entropy change at the standard state.

$\Delta G$  was calculated from the affinity constant ( $K_D$ ) using the equation  $\Delta G = RT \ln(K_D/C)$ , where  $R$  is 1.987 cal·mol<sup>-1</sup>K<sup>-1</sup>,  $K_D$  is expressed in mol/liter, and  $C$  is the standard state concentration (1 M).

The activation enthalpy of dissociation ( $\Delta^\ddagger H_d$ ) was determined by measuring  $k_{\text{off}}$  over a range of temperature (10–30 °C) and plotting  $\ln(k_{\text{off}}/T)$  against  $1/T$ , the slope of which equals  $-\Delta^\ddagger H_d/R$  (20).  $\Delta^\ddagger H_a$  was calculated from the relationship  $\Delta^\ddagger H_a = \Delta^\ddagger H_d + \Delta H$ .

In experiments varying the ionic strength a series of HBS stocks were prepared with the indicated NaCl or KF concentration. CD58 samples were diluted in the appropriate HBS buffer, and the same HBS buffer was used as the running buffer.

**Isothermal Titration Calorimetry**—ITC<sup>5</sup> measurements were performed at 25 °C using a MicroCal VP-ITC unit (MicroCal Inc.) as described previously (22). Samples were dialyzed extensively into HBS. CD58 at 245  $\mu\text{M}$  was injected in 10- $\mu\text{l}$  aliquots into a cell containing 1345  $\mu\text{l}$  of CD2 (at 35  $\mu\text{M}$ ), and the heat release was measured. The heat of dilution was obtained by injection of CD58 into HBS and subtracted prior to data analysis. The titration data were fitted by nonlinear curve fitting using Origin software, supplied with the instrument, to obtain the  $K_D$ , stoichiometry, and  $\Delta H$ .  $T\Delta S$  was determined by the relationship  $T\Delta S = \Delta H - RT \ln(K_D/C)$ .

## RESULTS AND DISCUSSION

**Thermodynamics of Human CD2 Binding to CD58**—To investigate whether CD2 binding to CD58 is accompanied by energetically significant conformational changes, we undertook a detailed thermodynamic analysis. The binding of CD58 to CD2 was analyzed by surface plasmon resonance. The affinity constant ( $K_D$ ) was measured by equilibrium binding analysis (10). The binding free energy of an interaction ( $\Delta G$ ), which can be calculated from the affinity constant (see “Experimental Procedures”), is comprised of enthalpic ( $\Delta H$ ) and entropic ( $-T\Delta S$ ) components ( $\Delta G = \Delta H - T\Delta S$ ).

The relative contribution of enthalpic and entropic components can be determined by measuring the dependence of  $\Delta G$  on temperature, a procedure termed van't Hoff analysis (see “Experimental Procedures”). For protein/protein interactions,  $\Delta H$  and  $T\Delta S$  typically vary with temperature, and this variation is measured as the change in heat capacity (at constant pressure) or  $\Delta C_p$ . The binding energy of the CD2/CD58 interaction was measured over the temperature range of 5 to 37 °C and  $\Delta H$ ,  $-T\Delta S$ , and  $\Delta C_p$  were determined by fitting the nonlinear form

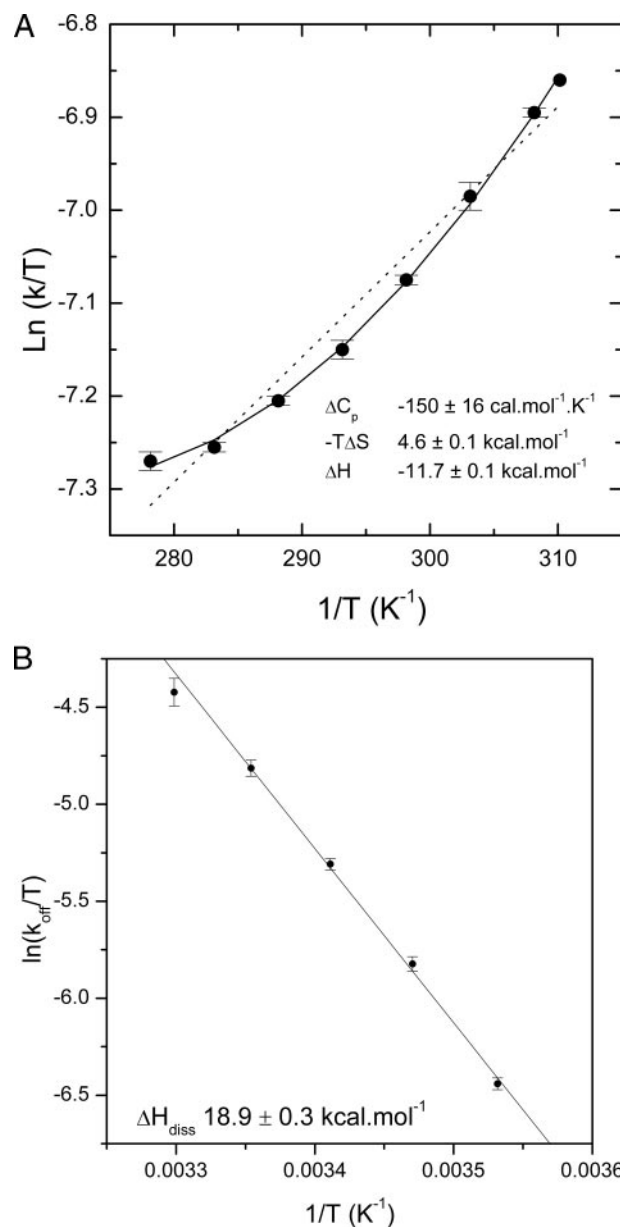


**FIGURE 1. Thermodynamic analysis of the CD2/CD58 interaction by surface plasmon resonance.** A, the  $K_D$  for the CD2/CD58 interaction was measured at the indicated temperatures converted into the standard state free energy change ( $\Delta G$ ). Values for  $\Delta H$ ,  $-T\Delta S$ , and  $\Delta C$  ( $\pm$ S.E. of fit) at 25 °C were derived by fitting the nonlinear form of the van't Hoff equation to the data (see “Experimental Procedures”). Also shown (as a dashed line) is a fit of the linear form of the van't Hoff equation where  $\Delta C = 0$ . B,  $k_{\text{off}}$  was measured at the indicated temperatures, and an Eyring plot was constructed (20), the slope of which yields  $\Delta^\ddagger H_d$  (see “Experimental Procedures”). The error bars indicate S.E. ( $n \geq 3$ ).

of the van't Hoff equation to the data (Fig. 1A). From several different determinations the  $\Delta H$  at 25 °C was determined to be  $-11.5 \pm 0.2$  kcal·mol<sup>-1</sup> (mean  $\pm$  S.E.,  $n = 3$ ), which is highly favorable. The corresponding entropic component ( $-T\Delta S$ ) was  $+4.4 \pm 0.2$  kcal·mol<sup>-1</sup>, which is unfavorable (Table 1).

$\Delta C_p$  determined by van't Hoff analysis was  $-118$  cal·mol<sup>-1</sup> K<sup>-1</sup> (Table 1). This falls at the high end of values typically reported for protein/protein interactions, which range from  $-1000$  to  $0$  cal·mol<sup>-1</sup> K<sup>-1</sup>, with an average value of approximately  $-300$  cal·mol<sup>-1</sup> K<sup>-1</sup> (23). A negative  $\Delta C_p$ , which is typ-

<sup>5</sup> The abbreviations used are: ITC, isothermal titration calorimetry; CD, cluster of differentiation;  $C_p$ , heat capacity at constant pressure; HBS, HEPES-buffered saline.

TABLE 1

Thermodynamic properties of the CD2/CD58 interaction

Parameter	Value <sup>a</sup>
$\Delta C_p$ (cal·mol <sup>-1</sup> K <sup>-1</sup> ) <sup>b</sup>	-118.0 ± 24
$\Delta C_p$ (calculated) <sup>c</sup>	-116.0 ± 1.4
$\Delta H_{VH}$ (kcal·mol <sup>-1</sup> ) <sup>b</sup>	-11.5 ± 0.2
$\Delta H_{ITC}$ <sup>d</sup>	-12.5 ± 0.02
$-T\Delta S_{VH}$ (kcal·mol <sup>-1</sup> ) <sup>b</sup>	4.4 ± 0.2
$-T\Delta S_{ITC}$ <sup>e</sup>	4.2 ± 0.1
$\Delta^{\ddagger}H_d$ (kcal·mol <sup>-1</sup> ) <sup>f</sup>	16.8 ± 0.6
$\Delta^{\ddagger}H_a$ <sup>g</sup>	5.3 ± 0.8

<sup>a</sup> Values shown are mean ± S.E. ( $n \geq 3$ ).  $\Delta C_p$  is assumed to be temperature-independent, and all other values are for 25 °C (298.15 K).

<sup>b</sup>  $\Delta C_p$ ,  $\Delta H_{VH}$ , and  $-T\Delta S_{VH}$  were measured by van't Hoff analysis (Fig. 1A).

<sup>c</sup> Calculated using the relationship  $\Delta C_{p(calc)} = (0.32 \pm 0.04) \Delta A_{np} - (0.14 \pm 0.04) \Delta A_p$ .

<sup>d</sup> Measured by isothermal titration calorimetry.

<sup>e</sup> Calculated from  $\Delta H_{ITC}$  and  $\Delta G$  measured by ITC (Fig. 2).

<sup>f</sup> Measured by Eyring analysis (Fig. 1B).

<sup>g</sup> Calculated from  $\Delta H_{VH}$  and  $\Delta^{\ddagger}H_d$ .

TABLE 2

Dissection of binding entropy ( $\Delta S$ )

Parameter	Value <sup>a</sup>
$\Delta S_{HE}$ (cal·mol <sup>-1</sup> K <sup>-1</sup> ) <sup>b</sup>	82.6
$\Delta S_{RT}$ (cal·mol <sup>-1</sup> K <sup>-1</sup> ) <sup>c</sup>	-50.0 (-8)
$\Delta S_{other}$ (cal·mol <sup>-1</sup> K <sup>-1</sup> ) <sup>d</sup>	-32.6 (-74.6)
$\mathfrak{R}$ <sup>e</sup>	6.0 (13)

<sup>a</sup> Determined for  $T = T_s = 261$  K, where  $\Delta S = 0$ .

<sup>b</sup>  $\Delta S_{HE} = 0.32 \Delta A_{np} \ln(T/386)$  with  $T = 261$  K.

<sup>c</sup>  $\Delta S_{RT}$  was assumed to be -50 (or -8) cal·mol<sup>-1</sup> K<sup>-1</sup>.

<sup>d</sup>  $\Delta S_{other}$  was calculated at  $T_s = 261$  K, where  $\Delta S = 0 = \Delta S_{other} + \Delta S_{HE} + \Delta S_{RT}$ . The value in parentheses assumes  $\Delta S_{RT} = -8$  cal·mol<sup>-1</sup> K<sup>-1</sup>.

<sup>e</sup>  $\mathfrak{R}$  was calculated using the equation  $\mathfrak{R} = \Delta S_{other}/-5.6$ . The value in parentheses assumes  $\Delta S_{RT} = -8$  cal·mol<sup>-1</sup> K<sup>-1</sup>.

ical of protein/protein interactions, is thought to be the result of the tendency of water to form an ordered "shell" adjacent to nonpolar surfaces which "melts" at higher temperatures (24). Upon binding, the burial of nonpolar surfaces disrupts this shell, ejecting the water into free solution, with favorable entropic and unfavorable enthalpic effects. Increasing the temperature melts the shell so that these effects are gradually lost. The relatively high  $\Delta C_p$  measured for the CD2/CD58 interaction is consistent with the fact that the binding interfaces are highly polar and that, as a result, a comparatively small amount of nonpolar surface is buried upon binding.

It is possible to estimate  $\Delta C_p$  from structural data using the empirically determined relationship

$$\Delta C_p = (0.32 \pm 0.04) \Delta A_{np} - (0.14 \pm 0.04) \Delta A_p \quad (\text{Eq. 1})$$

where  $\Delta A_{np}$  is the change in the buried nonpolar surface area and  $\Delta A_p$  is the change in the buried polar surface area. Using an implementation of the Lee and Richards algorithm developed by Hubbard (25–27),  $\Delta A_{np}$  and  $\Delta A_p$  were estimated from the crystal structure of the CD2/CD58 complex to be 660 and 690 Å<sup>2</sup>, respectively. Using these values, the calculated  $\Delta C_p$  is -116 cal·mol<sup>-1</sup> K<sup>-1</sup>, which is in good agreement with the experimental value obtained from van't Hoff analysis (Table 2).

Several studies have reported discrepancies between  $\Delta H$  measured indirectly by van't Hoff analysis ( $\Delta H_{VH}$ ) and  $\Delta H$  measured directly by calorimetry ( $\Delta H_{cal}$ ) (28–30). We therefore measured  $\Delta H$  directly using ITC (Fig. 2). The  $\Delta H$  and  $-T\Delta S$  thus measured were similar to those determined by van't Hoff analysis (Table 1). It has been suggested that differences between  $\Delta H_{cal}$  and  $\Delta H_{VH}$  indicate the presence of linked equilibria that contribute to  $\Delta H_{cal}$  but not  $\Delta H_{VH}$ . Recent studies

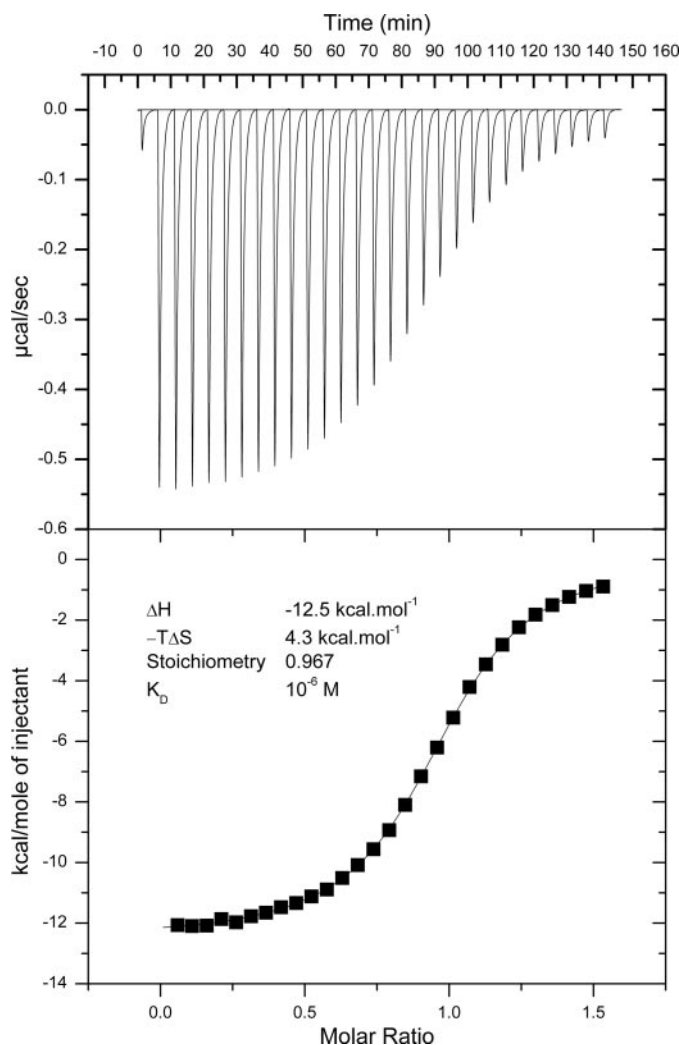


FIGURE 2. Thermodynamic analysis of the CD2/CD58 interaction by ITC.

The top panel shows the heat release during the titration of aliquots of CD58 into CD2 at 25 °C, corrected for base-line drift. The bottom panel shows the integrated heat of binding for the reaction plotted against the amount of injected CD58. These data were fitted to a single binding site model after subtracting the heat of dilution data, yielding the values shown for  $K_D$ , stoichiometry,  $\Delta H$ , and  $-T\Delta S$ . The fit S.E. values were <2%.

dispute this, however, arguing that  $\Delta H_{cal}$  should equal  $\Delta H_{VH}$  and that differences are more likely to be the result of experimental artifacts (31–33).

When conformational changes are required for binding, this may result in a high activation enthalpy of association ( $\Delta^{\ddagger}H_a$ ), which is a measure of the net number of bonds that need to be broken in order to form the transition state complex (34). Because the binding kinetics were too fast to measure the  $\Delta^{\ddagger}H_a$  directly, we determined the  $\Delta^{\ddagger}H_d$  and calculated the  $\Delta^{\ddagger}H_a$  from the relationship  $\Delta^{\ddagger}H_a = \Delta H + T\Delta^{\ddagger}H_d$ . We determined  $\Delta^{\ddagger}H_d$  by measuring the  $k_{off}$  over a range of temperatures (10–30 °C) and plotting  $\ln(k_{off}/T)$  against  $1/T$  (Fig. 1B), the slope of which equals  $-\Delta^{\ddagger}H_d/R$  (20). Using this approach the  $\Delta^{\ddagger}H_a$  thus estimated was  $5.3 \pm 0.8$  kcal·mol<sup>-1</sup>, which is relatively small (35). Although this does not support conformational change, it does not rule it out either, because it is possible that new bonds, such as long-range electrostatic interactions, are formed in the transition state that compensate for the bonds that are broken (36).



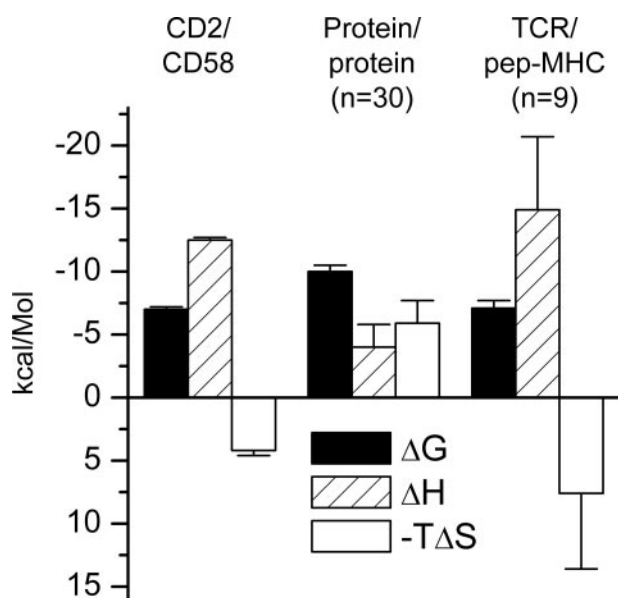


FIGURE 3. **Comparison of thermodynamics of protein/protein interactions.** Comparison of the thermodynamic parameters measured here for the CD2/CD58 interaction with the values (mean  $\pm$  S.D.) reported for 30 protein/protein (23) and nine T cell receptor (TCR)/peptide-loaded major histocompatibility complex (pep-MHC) (20, 47, 52–55) interactions.

The preponderance of charged residues in the binding interface supports this possibility, leading us to test (see below) whether long-range electrostatic interactions accelerate binding.

Our results show that, at physiological temperatures, the CD2/CD58 interaction is enthalpically driven and accompanied by unfavorable entropic changes. This contrasts with most protein/protein interactions (23), which are accompanied by favorable entropic and enthalpic changes (Fig. 3). It is similar to what has been observed with protein/protein interactions that are known to be accompanied by conformational adjustments and a reduction in conformational flexibility, such as T cell receptor/ligand (Fig. 3) and gp120/CD4 (37) interactions. However the unfavorable entropic change is relatively modest in comparison with these examples, and it is possible that it arises from sources other than changes in conformational flexibility. For example, it may arise purely from solvent effects, such as the trapping of water molecules in the binding interface. We therefore investigated the source of the unfavorable entropic change.

Entropic changes accompanying protein/protein interactions are the sum of favorable changes in solvent (water) entropy and unfavorable changes in protein entropy. Changes in solvent entropy arise mainly from the burial of nonpolar surfaces (*i.e.* the hydrophobic effect). This arises from the movement of water adjacent to hydrophobic surfaces, where it adopts an organized, shell-like structure, into free solution, where it is more disorganized. Changes in protein entropy arise from loss of rotational and translational freedom and conformational flexibility. To investigate the extent to which unfavorable entropic changes arise from changes in conformational flexibility, we used the approach suggested by Spolar and Record (38) to dissect total entropy change ( $\Delta S$ ) into three main components,

$$\Delta S = \Delta S_{\text{HE}} + \Delta S_{\text{RT}} + \Delta S_{\text{other}} \quad (\text{Eq. 2})$$

where  $\Delta S_{\text{HE}}$  is the entropy change associated with the hydrophobic effect,  $\Delta S_{\text{RT}}$  is the change associated with loss of translational and rotational freedom of the interacting proteins, and  $\Delta S_{\text{other}}$  is the change arising from other sources, including a reduction in conformational flexibility upon binding.  $\Delta S_{\text{HE}}$  arises from the burial of nonpolar surface area; it can be calculated from structural data using the empirically determined relationship

$$\Delta S_{\text{HE}} = 0.32 A_{\text{np}} \ln(T/386) \quad (\text{Eq. 3})$$

where  $A_{\text{np}}$  is the buried nonpolar surface area (in  $\text{\AA}^2$ ). As noted previously,  $A_{\text{np}}$  is estimated to be  $660 \text{ \AA}^2$  for the CD2/CD58 interaction.

Based on empirical measurements Spolar and Record (38) estimated  $\Delta S_{\text{RT}}$  to be  $-50 \text{ cal}\cdot\text{mol}^{-1}\text{K}^{-1}$  for a 1:1 protein/protein interaction. Because for protein/protein interactions  $\Delta S$  is temperature-dependent, there exists a temperature ( $T_s$ ) where  $\Delta S = 0$ . This can be calculated using the relationship

$$T_s = T^* e^{-\Delta S_T / \Delta C_p} \quad (\text{Eq. 4})$$

where  $T$  is an arbitrary temperature (*e.g.* 298.15 K) and  $\Delta S_T$  is the entropy change at that temperature. Using the  $\Delta S_T$  and  $\Delta C_p$  values determined above,  $T_s$  was calculated to be 261 K for the CD2/CD58 interaction.  $\Delta S_{\text{HE}}$  at  $T_s$  was calculated using Equation 3 to be  $83 \text{ cal}\cdot\text{mol}^{-1}\text{K}^{-1}$ .

$\Delta S_{\text{other}}$  at  $T_s$  can thus be calculated from the relationship

$$\Delta S = 0 = \Delta S_{\text{other}} + \Delta S_{\text{HE}} + \Delta S_{\text{RT}} \quad (\text{Eq. 5})$$

If one assumes that  $\Delta S_{\text{RT}}$  is temperature-independent over this temperature range, as suggested by Spolar and Record (38), then  $\Delta S_{\text{other}}$  is calculated to be  $-33 \text{ cal}\cdot\text{mol}^{-1}\text{K}^{-1}$  (Table 2). This negative  $\Delta S_{\text{other}}$  value indicates that binding is accompanied by a reduction in conformational entropy. Spolar and Record (38) show that the number of residues ( $\mathfrak{R}$ ) undergoing the transition from a flexible to a folded or rigid state can be estimated from the empirical relationship

$$\mathfrak{R} = \Delta S_{\text{other}} / -5.6 \quad (\text{Eq. 6})$$

suggesting that  $\sim 6$  or more residues are converted from a flexible to a stable state upon CD2 binding to CD58.

Recently it has been argued that a better estimate of  $\Delta S_{\text{RT}}$  for protein/protein association would be the cratic entropy (39), which is  $-8 \text{ cal}\cdot\text{mol}^{-1}\text{K}^{-1}$  ( $R \ln 1/55.5$ ) for a bimolecular interaction in water in the standard state. Substituting this value into Equation 5 would give  $-74.6 \text{ cal}\cdot\text{mol}^{-1}\text{K}^{-1}$  for  $\Delta S_{\text{other}}$  and substituting this in Equation 6 gives a value of 13 for  $\mathfrak{R}$  (Table 2). Thus dissection of the binding entropy suggests that CD2 binding to CD58 is accompanied by a reduction in conformational flexibility involving 6–13 residues. Although these changes might occur anywhere in the protein complex, structural studies support the notion that this reduction in conformational flexibility involves the BC, C'C'', and FG loops of CD2 (16, 17) and the C'C'' and FG loops of CD58 (14). As noted above, CD2 binding to CD58 is accompanied by and driven by a large, favorable enthalpy change. Such favorable enthalpy changes may arise from an increased number of contacts forming at the interface and/or from the trapping of solvent within

the binding interface. The binding interface of the CD2/CD58 complex is  $\sim 1150 \text{ \AA}^2$  (14). Although this is at the low end of the range for protein/protein interactions (23, 41), there appear to be numerous contacts; 10 salt bridges and five hydrogen bonds were proposed based on analysis of the crystal structure (14). Site-directed mutagenesis studies of the CD2/CD58 interaction suggest that a centrally positioned CD2 tyrosine and surrounding charged residues make major contributions to the binding energy (42–45). Interestingly, the CD2/CD58 binding interface exhibits poor surface shape complementarity (14), suggesting that water molecules bridge the binding surfaces and raising the possibility that trapped water contributes to the favorable enthalpy changes.

**Effect of Electrostatic Interactions on CD2 Binding to CD58—**Proteins typically associate in solution with a rate constant of  $10^5$ – $10^6 \text{ M}^{-1}\text{s}^{-1}$  (36, 46). This rate may decrease if binding requires conformational adjustments (37, 47). Given the evidence from structural and thermodynamic studies that CD2 binding to CD58 is accompanied by conformational change, it is notable that the association rate constant of the CD2/CD58 interaction is not particularly slow ( $k_{\text{on}} \geq 4 \times 10^5 \text{ M}^{-1}\text{s}^{-1}$ ) (10). The association may be accelerated, sometimes dramatically (48), by favorable long-range electrostatic interactions. The mechanism is believed to involve accelerated collisions and/or steering proteins into the correct orientation for binding (36, 46, 49). Given that the CD2/CD58 binding interface is highly charged (14), we investigated the contribution of long-range electrostatic interactions to binding by examining the effect of varying solution ionic strength.

We initially varied the ionic strength by changing the NaCl concentration. Increasing the NaCl concentration from 150 to 1500 mM resulted in an  $\sim 6$ -fold decrease in affinity (Fig. 4A), consistent with a previous report (43). This effect was primarily a result of an effect on the  $k_{\text{on}}$  (Fig. 4B), consistent with screening of long-range electrostatic interactions. Recent studies have shown that electrostatic screening results in a linear relationship between  $\ln k_{\text{on}}$  and  $1/(1 + \kappa a)$ , where the latter is proportional to the ionic strength (36). In the case of the CD2/CD58 interaction, this relationship was clearly not linear (Fig. 4C), suggesting that the effect of NaCl was not solely the result of electrostatic screening. One possible explanation was that the sodium and/or chloride ions were disrupting the structure of CD2 and/or CD58 either by direct interactions with the proteins or through effects on solvent structure. Because such effects are dependent on the salt, we used a different salt (KF) to vary the ionic strength. In contrast to the effect of NaCl, the affinity and kinetics of CD2 binding to CD58 showed no significant change when the concentration of KF was varied from 150 to 1500 mM (Fig. 4). It follows that the effect of varying NaCl on binding is not the result of changes in ionic strength and must result from another mechanism. Interestingly, the rat CD2/CD48 interaction was unaffected by varying the NaCl concentration (50), implying that rat CD2 and/or CD48 are resistant to this effect. Given that the surface charge distributions on CD2/ligand binding surfaces are not conserved across species and that the ligand binding surfaces of the human CD2/ligand pair are more highly charged, it is not surprising that they exhibit differential sensitivity to NaCl (12, 14).

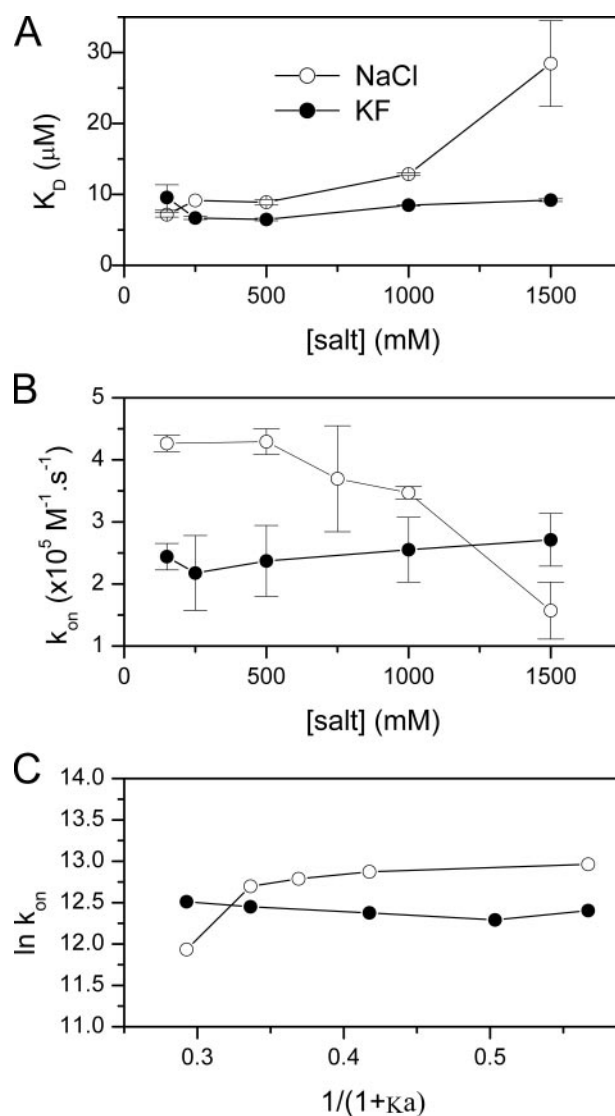


**FIGURE 4. The dependence of binding on ionic strength.** The dependence of  $K_D$  (A), and  $k_{\text{on}}$  (B and C) on the concentration of NaCl or KF (40) is shown. The  $K_D$  was measured directly, whereas  $k_{\text{on}}$  was calculated from the relationship  $k_{\text{on}} = k_{\text{off}}/K_D$  following direct measurement of  $k_{\text{off}}$ . The error bars indicate S.E. ( $n \geq 3$ ) and were determined by error propagation for  $k_{\text{on}}$ .

The absence of an effect when varying KF concentration demonstrates that long-range electrostatic interactions have no net effect on the CD2/CD58 interaction. This is somewhat unexpected given that the binding interfaces in the complex are highly charged with excellent charge complementarity (14). However, it remains possible that there are some favorable electrostatic interactions that are balanced by unfavorable electrostatic interactions. To investigate this further we used site-directed mutagenesis to disrupt a subset of electrostatic interactions. We had recently generated a number of human CD2 mutants in which single charged residues in the binding interface were mutated to alanine (18). Because it was not possible directly to measure  $k_{\text{on}}$ , we calculated it from the  $K_D$  and  $k_{\text{off}}$  (Table 3). Although mutation of CD2 residues Lys<sup>41</sup>, Lys<sup>51</sup>, and Lys<sup>91</sup> to alanine had no significant effect on the  $k_{\text{on}}$ , mutation of Asp<sup>31</sup> to alanine led to a 5-fold decrease in the  $k_{\text{on}}$  value from  $4 \times 10^5$  to  $0.8 \times 10^5 \text{ M}^{-1}\text{s}^{-1}$  (Table 3). Interestingly, Asp<sup>31</sup>

**TABLE 3****Effect of CD2 mutations on association rate constant**

As the binding kinetics were too fast to allow direct measurement,  $k_{on}$  was calculated using the relationship  $k_{on} = k_{off}/K_D$  and previously determined values for  $k_{off}$  and  $K_D$  at 25 °C (18). Values shown are mean  $\pm$  S.E. ( $n \geq 3$ ) with the S.E. calculated by error propagation from  $k_{off}$  and  $K_D$  S.E. values.

Mutation	$k_{on}$ $M^{-1} s^{-1}$
Wild type	$4.0 \pm 0.4 \times 10^5$
K41A	$2.3 \pm 0.3 \times 10^5$
K51A	$4.2 \pm 0.4 \times 10^5$
K91A	$3.1 \pm 0.3 \times 10^5$
D31A	$0.8 \pm 0.2 \times 10^5$

forms a salt bridge with the CD58 residue Arg<sup>44</sup> in the bound complex (14). Taken together, these data suggest that a favorable electrostatic interaction involving Asp<sup>31</sup> and Arg<sup>44</sup> accelerates CD2 binding to CD58 but that other, unfavorable interactions inhibit association. Interestingly, there is also evidence that the rat CD2/CD48 interaction is also characterized by balancing unfavorable and favorable electrostatic interactions; whereas this interaction is unaffected by changes in salt concentration, mutation to alanine of individual charged residues in the binding interface resulted in both decreases and increases in affinity (50).

Given the highly charged nature of the CD2/CD58 binding interface, our finding that long-range electrostatic interactions do not accelerate binding is unexpected and in striking contrast to the barnase/barstar interaction, where electrostatic attractions between highly charged surfaces accelerate binding by several orders of magnitude (48). One difference between the CD2/CD58 and barnase/barstar interfaces is that the latter is less heterogeneous; barnase is predominantly positively charged, and barstar is uniformly negatively charged. In contrast, the CD2 and CD58 binding surfaces each carry an intricate mixture of negative and positive charges (12, 14). We suggest that the presence of heterogeneous charges on each surface results in a complex electrostatic potential energy landscape with a balancing of favorable and unfavorable long-range electrostatic interactions. Given that it has no effect on binding kinetics, what is the functional significance of charged nature of the CD2/CD58 binding interface? We have shown previously, in an analysis of the rat CD2/CD48 interaction, that charged residues that contribute little to the binding affinity may nevertheless contribute to binding specificity by imposing a requirement for charge complementarity on the other surface (50). The reason proposed for their small contribution to affinity is that, in order for them to form favorable interactions (e.g. salt bridges) with the ligand, existing favorable electrostatic interactions (e.g. with water, salt, or adjacent residues) need to be broken. The molecular interactions that mediate transient cell/cell interactions need to be low affinity to facilitate detachment. We suggest that the CD2/CD58 binding interface is charged because electrostatic complementarity enables the interaction to be both weak and specific.

**Conclusion**—In this report we have shown that the CD2/CD58 interaction is accompanied by an unfavorable entropy change. Dissection of the entropy change using the approach of Spolar and Record (38) suggests that the unfavorable entropy change results in part from a reduction in conformational flex-

ibility. Taken together with previous structural studies, these findings suggest that energetically significant structural rearrangements accompany binding. Despite the highly charged binding interface, we have shown that long-range electrostatic interactions have no net favorable effect on CD2 binding to CD58, probably because of the presence of balancing favorable and unfavorable electrostatic interactions.

**Acknowledgments**—We thank Neil Barclay for valuable advice, Jennifer Byrne for assistance with tissue culture, and David Mahoney and Anthony Day for assistance with ITC measurements.

**REFERENCES**

- Davis, S. J., and van der Merwe, P. A. (1996) *Immunol. Today* **17**, 177–187
- Engel, P., Eck, M. J., and Terhorst, C. (2003) *Nat. Rev. Immunol.* **3**, 813–821
- Bachmann, M. F., Barner, M., and Kopf, M. (1999) *J. Exp. Med.* **190**, 1383–1392
- Bierer, B. E., and Burakoff, S. J. (1989) *Immunol. Rev.* **111**, 267–294
- Green, J. M., Karpitskiy, V., Kimzey, S. L., and Shaw, A. S. (2000) *J. Immunol.* **164**, 3591–3595
- Moingeon, P., Chang, H. C., Sayre, P. H., Clayton, L. K., Alcover, A., Gardner, P., and Reinherz, E. L. (1989) *Immunol. Rev.* **111**, 111–144
- van der Merwe, P. A. (1999) *J. Exp. Med.* **190**, 1371–1374
- Davis, S. J., Ikemizu, S., Wild, M. K., and van der Merwe, P. A. (1998) *Immunol. Rev.* **163**, 217–236
- van der Merwe, P. A., and Davis, S. J. (2003) *Annu. Rev. Immunol.* **21**, 659–684
- van der Merwe, P. A., Barclay, A. N., Mason, D. W., Davies, E. A., Morgan, B. P., Tone, M., Krishnam, A. K., Ianelli, C., and Davis, S. J. (1994) *Biochemistry* **33**, 10149–10160
- Bodian, D. L., Jones, E. Y., Stuart, D. I., Harlos, K. H., Davies, E. A., and Davis, S. J. (1994) *Structure (Lond.)* **2**, 755–766
- Ikemizu, S., Sparks, L. M., van der Merwe, P. A., Harlos, K., Stuart, D. I., Jones, E. Y., and Davis, S. J. (1999) *Proc. Natl. Acad. Sci. U. S. A.* **96**, 4289–4294
- Sun, Z. Y., Dötsch, V., Kim, M., Li, J., Reinherz, E. L., and Wagner, G. (1999) *EMBO J.* **18**, 2941–2949
- Wang, J. H., Smolyar, A., Tan, K., Liu, J. H., Kim, M., Sun, Z. Y., Wagner, G., and Reinherz, E. L. (1999) *Cell* **97**, 791–803
- Wyss, D. F., Choi, J. S., Jing, L., Knoppers, M. H., Willis, K. J., Arulanandam, A. R. N., Reinherz, E. L., and Wagner, G. (1995) *Science* **269**, 1273–1278
- Kitao, A., and Wagner, G. (2000) *Proc. Natl. Acad. Sci. U. S. A.* **97**, 2064–2068
- Wyss, D. F., Dayie, K. T., and Wagner, G. (1997) *Protein Sci.* **6**, 534–542
- Bayas, M. V., Kearney, A., Avramovic, A., van der Merwe, P. A., and Leckband, D. E. (2007) *J. Biol. Chem.* **282**, 5589–5596
- Karlsson, R., and Ståhlberg, R. (1995) *Anal. Biochem.* **228**, 274–280
- Lee, J. K., Stewart-Jones, G., Dong, T., Harlos, K., Di Gleria, K., Dorrell, L., Douek, D. C., van der Merwe, P. A., Jones, E. Y., and McMichael, A. J. (2004) *J. Exp. Med.* **200**, 1455–1466
- Yoo, S. H., and Lewis, M. S. (1995) *Biochemistry* **34**, 632–638
- Ladbury, J. E., and Chowdhry, B. Z. (1996) *Chem. Biol.* **3**, 791–801
- Stites, W. E. (1997) *Chem. Rev.* **97**, 1233–1250
- Creighton, T. (1993) *Proteins. Structures and Molecular Properties*, 2nd Ed., pp. 157–160, W. H. Freeman, New York
- Lee, B., and Richards, F. M. (1971) *J. Mol. Biol.* **55**, 379–400
- McDonald, I. K., and Thornton, J. M. (1994) *J. Mol. Biol.* **238**, 777–793
- Laskowski, R. A. (1995) *J. Mol. Graph.* **13**, 323–330, 307–328
- Naghibi, H., Tamura, A., and Sturtevant, J. M. (1995) *Proc. Natl. Acad. Sci. U. S. A.* **92**, 5597–5599
- Sigurskjöld, B. W., and Bundle, D. R. (1992) *J. Biol. Chem.* **267**, 8371–8376
- Liu, Y., and Sturtevant, J. M. (1995) *Protein Sci.* **4**, 2559–2561
- Horn, J. R., Russell, D., Lewis, E. A., and Murphy, K. P. (2001) *Biochemistry*



- 40, 1774–1778
32. Horn, J. R., Brandts, J. F., and Murphy, K. P. (2002) *Biochemistry* **41**, 7501–7507
33. Chaires, J. B. (1997) *Biophys. Chem.* **64**, 15–23
34. Atkins, P. (1998) *Physical Chemistry*, pp. 830–833, Oxford University Press, Oxford
35. Gutfreund, H. (1995) *Kinetics for the life Sciences. Receptors, Transmitters, and Catalysis*, pp. 231–280, Cambridge University Press, Cambridge
36. Schreiber, G. (2002) *Curr. Opin. Struct. Biol.* **12**, 41–47
37. Myszk, D. G., Sweet, R. W., Hensley, P., Brigham-Burke, M., Kwong, P. D., Hendrickson, W. A., Wyatt, R., Sodroski, J., and Doyle, M. L. (2000) *Proc. Natl. Acad. Sci. U. S. A.* **97**, 9026–9031
38. Spolar, R. S., and Record, M. T., Jr. (1994) *Science* **263**, 777–784
39. Murphy, K. P., Xie, D., Thompson, K. S., Amzel, L. M., and Freire, E. (1994) *Proteins* **18**, 63–67
40. Shogren, R. L., Jamieson, A. M., Blackwell, J., and Jentoft, N. (1986) *Biopolymers* **25**, 1505–1517
41. Lo Conte, L., Chothia, C., and Janin, J. (1999) *J. Mol. Biol.* **285**, 2177–2198
42. Arulanandam, A. R. N., Withka, J. M., Wyss, D. F., Wagner, G., Kister, A., Pallai, P., Recny, M. A., and Reinherz, E. L. (1993) *Proc. Natl. Acad. Sci. U. S. A.* **90**, 11613–11617
43. Kim, M., Sun, Z. Y., Byron, O., Campbell, G., Wagner, G., Wang, J., and Reinherz, E. L. (2001) *J. Mol. Biol.* **312**, 711–720
44. Arulanandam, A. R. N., Kister, A., McGregor, M. J., Wyss, D. F., Wagner, G., and Reinherz, E. L. (1994) *J. Exp. Med.* **180**, 1861–1871
45. Somoza, C., Driscoll, P. C., Cyster, J. G., and Williams, A. F. (1993) *J. Exp. Med.* **178**, 549–558
46. Janin, J. (1997) *Proteins* **28**, 153–161
47. Willcox, B. E., Gao, G. F., Wyer, J. R., Ladbury, J. E., Bell, J. I., Jakobsen, B. K., and van der Merwe, P. A. (1999) *Immunity* **10**, 357–365
48. Schreiber, G., and Fersht, A. R. (1996) *Nat. Struct. Biol.* **3**, 427–431
49. Sheinerman, F. B., Norel, R., and Honig, B. (2000) *Curr. Opin. Struct. Biol.* **10**, 153–159
50. Davis, S. J., Davies, E. A., Tucknott, M. G., Jones, E. Y., and van der Merwe, P. A. (1998) *Proc. Natl. Acad. Sci. U. S. A.* **95**, 5490–5549
51. Deleted in proof
52. Anikeeva, N., Lebedeva, T., Krogsgaard, M., Tetin, S. Y., Martinez-Hackert, E., Kalams, S. A., Davis, M. M., and Sykulev, Y. (2003) *Biochemistry* **42**, 4709–4716
53. Davis-Harrison, R. L., Armstrong, K. M., and Baker, B. M. (2005) *J. Mol. Biol.* **346**, 533–550
54. Garcia, K. C., Radu, C. G., Ho, J., Ober, R. J., and Ward, E. S. (2001) *Proc. Natl. Acad. Sci. U. S. A.* **98**, 6818–6823
55. Krogsgaard, M., Prado, N., Adams, E. J., He, X. L., Chow, D. C., Wilson, D. B., Garcia, K. C., and Davis, M. M. (2003) *Mol. Cell* **12**, 1367–1378

**The Contribution of Conformational Adjustments and Long-range Electrostatic Forces to the CD2/CD58 Interaction**

Alice Kearney, Adam Avramovic, Mónica A. A. Castro, Alexandre M. Carmo, Simon J. Davis and P. Anton van der Merwe

*J. Biol. Chem.* 2007, 282:13160-13166.

doi: 10.1074/jbc.M700829200 originally published online March 7, 2007

---

Access the most updated version of this article at doi: [10.1074/jbc.M700829200](https://doi.org/10.1074/jbc.M700829200)

Alerts:

- [When this article is cited](#)
- [When a correction for this article is posted](#)

[Click here](#) to choose from all of JBC's e-mail alerts

This article cites 51 references, 17 of which can be accessed free at <http://www.jbc.org/content/282/18/13160.full.html#ref-list-1>